2

Conf-9308181--3

UCRL-JC-115918
PREPRINT

The PHENIX Experiment at RHIC

S. R. Tonse
J. H. Thomas

This paper was prepared for submittal to the
Proceedings of the workshop on Pre-Equilibrium Parton Dynamics
Berkeley, CA
August 23-September 3, 1993

December 15, 1993

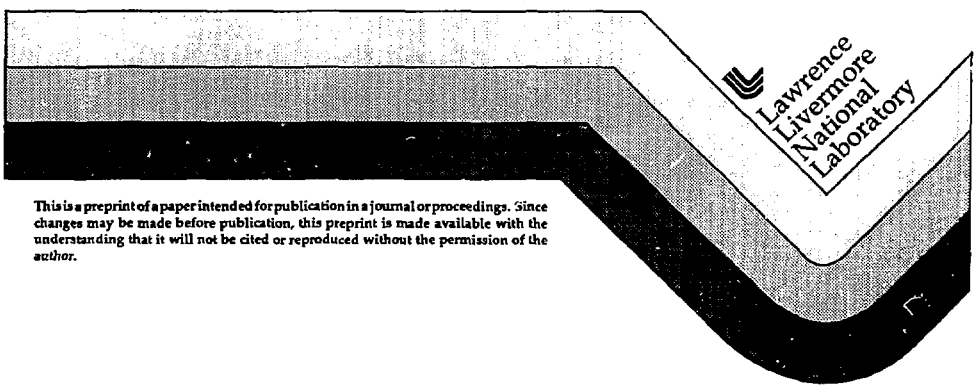

THE PHENIX EXPERIMENT AT RHIC

S.R.Tonse and J.H.Thomas

N Division, L-397,
Lawrence Livermore National Laboratory,
P.O.Box 808, Livermore, CA 94550

Abstract

Later this decade the Relativistic Heavy Ion Collider (RHIC) will be built at Brookhaven Natl. Lab. Its goal will be to accelerate and collide Au beams at 100 GeV/c in an attempt to create a Quark Gluon Plasma (QGP). The PHENIX detector aims to detect the QGP through its leptonic and hadronic signatures. We describe here its physics capabilities and the details of the apparatus designed to pick out rare leptonic signatures from among hadronic multiplicities of up to 1500 particles per unit of rapidity.

INTRODUCTION

Many experimental signatures for the QGP have been proposed, both hadronic and leptonic in nature. The advantage of leptons is that they emerge from the plasma untouched and give a direct picture of events that have happened in the plasma itself. Hadronic signatures are more indirect, since they are affected by what happens as the plasma cools and hadronizes, and emerging hadrons will themselves have interactions. Phenix aims to look for purely leptonic signatures, purely hadronic ones, and for hadronic signatures through leptonic measurements. The detector is being designed to measure electrons, muons, charged hadrons, and photons. With these data we will study single charged particle production rates, compare production of strange to non-strange hadrons, study production and possible mass-shifts of vector mesons through their leptonic decays to electron pairs and muon pairs, look at thermally produced electron pairs, and search for an enhancement of the direct photon production expected in a plasma from abundant $q\bar{q}$ annihilation. This search is not intended to be done with exclusive measurements, (ie. event by event) since some

of the leptonic signatures are rare and rates are insufficient for this. Instead we will take a semi-inclusive route and characterize and classify events through calorimetry, multiplicity, and the energy and identity of the incident colliding systems. We will then search for simultaneous occurances of several of the QGP signatures in these different event classes. To identify and separate electrons from the more plentiful hadrons, Phenix is using a varied array of detector technologies with strengths in different kinematic regions.

Phenix currently has > 300 collaborators from universities and national laboratories throughout the United States, and from Brazil, Canada, China, Germany, India, Japan, Korea, Russia and Sweden.

PHYSICS

Table 1 summarizes the PHENIX physics agenda. The probes PHENIX will use to study the QGP include electrons, photons, and muons.

Thermal electrons are formed by $q\bar{q}$ annihilation and emerge as a dilepton pair[1]. The rate of production is predicted to have a strong dependence on the plasma "temperature", which can be extracted from the slope of the p_T sum of the pair. But there are relatively few electrons among the numerous hadrons produced in an ultra-relativistic heavy ion collision and so Phenix requires electron/pion separation capabilities of approximately 1 part in 10,000. Also, there are 10 to 20 electrons/event from "background" sources such as $\pi^0 \rightarrow \gamma e^+e^-$ (Dalitz) decay and photon conversion $\gamma \rightarrow e^+e^-$. *Measuring the dilepton spectrum is therefore difficult* at invariant masses below 700 MeV/c^2 because the combinatoric background from the Dalitz electron pairs dominates. The optimum p_T interval for measuring the vector meson resonances is between 1 and 3 GeV/c^2.

We are looking for the ρ, ω,ϕ, and J/ψ mesons via their decays to e^+e^- and $\mu^+\mu^-$. These decay modes are not prime modes for any of these mesons and typically have branching ratios of 0.01% except for the J/ψ. The need to capture both of the decay products is what dictated Phenix's appearance, with two arms 135° apart in azimuthal angle. Of the vector mesons, the ϕ is the most interesting since in addition to the possibility of QGP formation there is a prediction that chiral symmetry restoration may occur and we could see this through the change in the strange quark masses and the resulting mass shift of the ϕ meson [2]. We will be able to detect such a change in the position of the narrow ϕ mass peak. Also since the Q-value of the $\phi \rightarrow KK$ channel is so small, a change in Kaon masses would strongly affect *the ϕ decay rate*, which would manifest itself as a change in the width of the mass peak. Being able to resolve this is one of the main issues driving the tracking system design. Strange quark production [3] is another quantity that can be measured through the ϕ, by comparing , say, the production of $\phi/(\rho + \omega)$. The J/ψ production [4] is sensitive to the Debye screening length of the plasma, and QGP formation is expected to result in a suppression of J/ψ production. Phenix will primarily look at this through the $\mu^+\mu^-$ decay, (although some e^+e^- decays will be visible). The heavier ψ' and the Υ

Table 1: Physics issues to be addressed by the PHENIX detector.

QGP Physics Issues	Probes
Debye Screening of QCD Interactions	
• $r(\Upsilon) = 0.13$ fm $< r(J/\psi) = 0.29$ fm $< r(\psi') = 0.56$ fm	
$J/\psi \rightarrow e^+e^-$ at $y \simeq 0$.	Electrons
$J/\psi \rightarrow \mu^+\mu^-$ at $y \simeq 2$.	
$\psi', \Upsilon \rightarrow \mu^+\mu^-$ at $y \simeq 2$.	Muons
Chiral Symmetry Restoration	
• Mass, Width, Branching Ratio: $\phi \rightarrow e^+e^-$, K^+K^-	Electrons
with $\Delta m \leq 5$ MeV.	Hadrons
• Baryon Susceptibility: Production of antinuclei.	
• Narrow σ-meson?	
Thermal Radiation of Hot Gas	
• Prompt γ, Prompt $\gamma^* \rightarrow e^+e^-$.	γ, Electrons
Deconfinement: Nature of the Phase Transition	
• First-order: Entropy Jump $\rightarrow$ Second rise in the $< p_T >$	Hadrons
spectra of π, K, p.	
• Second-order: Fluctuation $\rightarrow N(\pi^0)/N(\pi^+ + \pi^-), d^2N/d\eta d\phi$.	Hadrons, γ
Strangeness and Charm Production	
• Production of K^+, K^-, K^0_L.	Hadrons
$\phi \rightarrow e^+e^-$, K^+K^- at $y \simeq 0$,	Electrons
$\phi \rightarrow \mu^+\mu^-$ at $y \simeq 2$.	Muons
D-meson: $e\mu$ coincidence.	
Jet Quenching	
• High p_T jets via eading particle spectra.	Hadrons
Space-Time Evolution	
• HBT correlations for $\pi\pi$ and KK.	Hadrons

mesons will also be seen through the muon decay channels. Since all of these mesons have different radii, their production rate should be affected to different degrees by the Debye screening.

Photon production in heavy ion collisions comes from several sources, depending on the kinematics of the photon. Several of these are of interest. At high p_T (>5 GeV/c) photons from hard scattering of initial state quarks are expected. At slightly lower values (p_T ~2-5 GeV/c) photons from pre-equilibrium collisions, and from (p_T ~0.5-2 GeV/c) emission of photons from a thermalized plasma is expected to be significant. These signals must be separated from the background of $\pi^0 \rightarrow \gamma\gamma$ decay, and will then yield information on the initial plasma temperature, as well as on the plasma critical temperature.[5]

Measurement of QGP signatures of a hadronic nature in conjunction with leptonic signatures is desirable. For hadronic measurements Phenix will study single particle

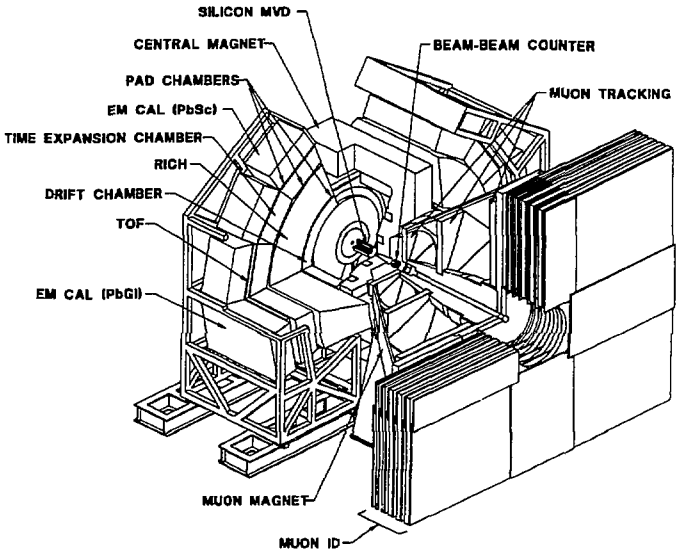

Figure 1: Isometric view of the PHENIX detector.

spectra to search for a rise in the mean particle p_T, indicative of a first-order phase transition, two-particle Bose-Einstein correlations to determine formation time plus the size of the interaction region, and strangeness production, through Kaon and ϕ (through $\phi \rightarrow K^+K^-$) production.

DETECTORS

The PHENIX detector is shown in Figures 1 and 2. The detector will be located in RHIC's Major Facility Hall. It has two central arms, centered about the collision region, for detection of electrons, photons and hadrons, and a muon detection arm at higher rapidity. These two divisions operate more or less independently of each other, with separate sub-detectors and magnets.

The central arms view central rapidities, with a field of $\eta = \pm 0.35$, and 90° of azimuthal coverage each. A magnetic field (described in next section) extends from the beamline out to a radius of ≈3m. The detector components of the central arms are outside the field (or in its fringes) and consist of drift chambers, pad chambers,

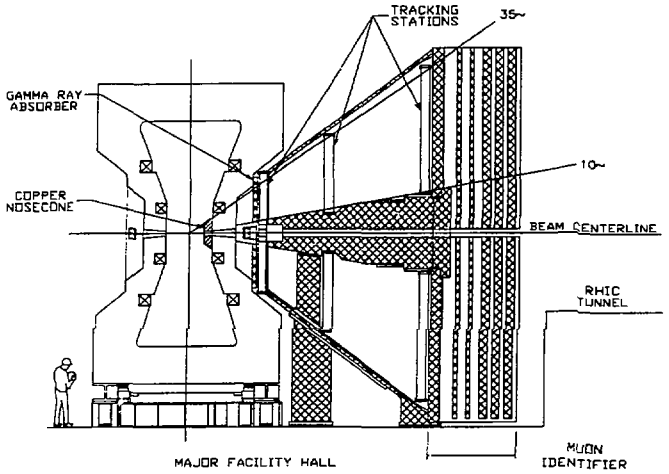

Figure 2: Side view of PHENIX with the Central Magnet detector array removed.

a time expansion chamber (TEC) (these 3 are collectively referred to as the tracking system), a Ring-Imaging Cerenkov detector (RICH), an Electromagnetic Calorimeter (EMCal) and a scintillator-based Time of Flight (TOF) system. Each of these systems has a strength, be it accuracy in track reconstruction, particle identification, low occupancy rate (hence an ability to reduce the number of tracking ambiguities for another detector), or a fast time response (making it attractive to use from a triggering point of view). Figure 3 and Table 2 show these detectors in order of increasing radius, and summarizes their functionality. Our intention is for these detectors to work together, combining their strengths to provide either track reconstruction information, particle identification, or both, over a wide range of particle momenta.

The muon arm views higher rapidities, covering θ from 10° to 35° in polar angle, and consists of several tracking detectors, and a streamer-tube based muon identifier. It has its own magnet system, and uses the central magnet pole-face as a particle filter that allows muons to pass through while stopping a large fraction of the hadrons.

Magnets:

Central Magnet: The magnet system for the central arms provides an axially symmetric magnetic field parallel to the beamline, by means of two pairs of Helmholtz coils. Two inner coils have radii of $\approx$0.75m and are placed at z=$\pm$0.6m from the central collision point, and perpendicular to the beamline. The two outer coils have radii of $\approx$1.75m and are placed at z=$\pm$1.0m. The reason for two pairs of coils instead

of just one is to allow for the possibility of running them either with their fields adding or opposing. In the latter mode, there will be a field-free region from the beamline to about 1m radius, which we would use to identify electron pairs that arise from π^0 Dalitz decay, a major source of background. Since Dalitz pairs are produced with a small opening angle a field-free region would result in their emerging unseparated and we could identify them by looking for e^+e^- pairs close together. The actual construction of the inner coils has been deferred and Phenix will start up with only the outer coils. The magnetic field will primarily have only a z component, with an integrated field strength of 0.78 Tesla-meters. The radial profile of B_z is approximately Gaussian with FWHM=2.65m.

Muon Magnet: The muon magnet system starts immediately behind one of the central magnet pole-faces. The prominent feature here is a large 400 ton steel piston 4m long, stretching from z=2m to z=6m from the collision point, and tapered, having radius 0.35m at the small end and r=1m at the large end. Two coils are wound around the piston causing a solenoidal B field to flow through it along the z direction. Part of this field radiates away from the piston creating a radial B field with a field

Table 2: Phenix detector parameters

Detector	Solid Angle		Radial Allocation (cm)	Spatial Resoluion	2-Particle Resolution
	$\Delta\eta$	$\Delta\phi$			
BBC	±3.1-4.0	360°	-	25mm	-
MVD	±2.7	360°	5-20	0.2mm (z)	-
DC	±0.35	90° + 90°	205.0-245.0	0.15mm (rϕ)	1.5mm
PC1	±0.35	90° + 90°	247.5-252.5	2mm (rϕ) 2mm (z)	8mm (rϕ) 8mm (z)
RICH	±0.35	90° + 90°	257.5-410.0	1°θ, 1°ϕ	2°θ, 2°ϕ
PC2	±0.35	90° + 90°	415.0-421.0	3mm (rϕ) 3mm (z)	12mm (rϕ) 12mm (z)
TEC	±0.35	90° + 90°	421.7-491.0	0.25mm (rϕ)	4mm (rϕ) 5mm (z)
PC3	±0.35	90° + 90°	491.0-498.0	4mm (rϕ) 4mm (z)	16mm (rϕ) 16mm (z)
TOF	±0.35	30°	503.0-518.0	15mm (rϕ) 15mm (z)	15mm(z)
EMCal Pb-Sc	±0.35	90° + 45°	503.0-593.0	8mm @ 1 GeV	70mm
EMCal Pb-Gl	±0.35	45°	523.0-613.0	6mm @ 1 GeV	50mm
Muon Trck.	1.15-2.35	360°	-	0.2mm	1.5mm
Muon ID	1.15-2.35	360°	-	1°ϕ 5.6°θ	2°(ϕ) 11.2°(θ)

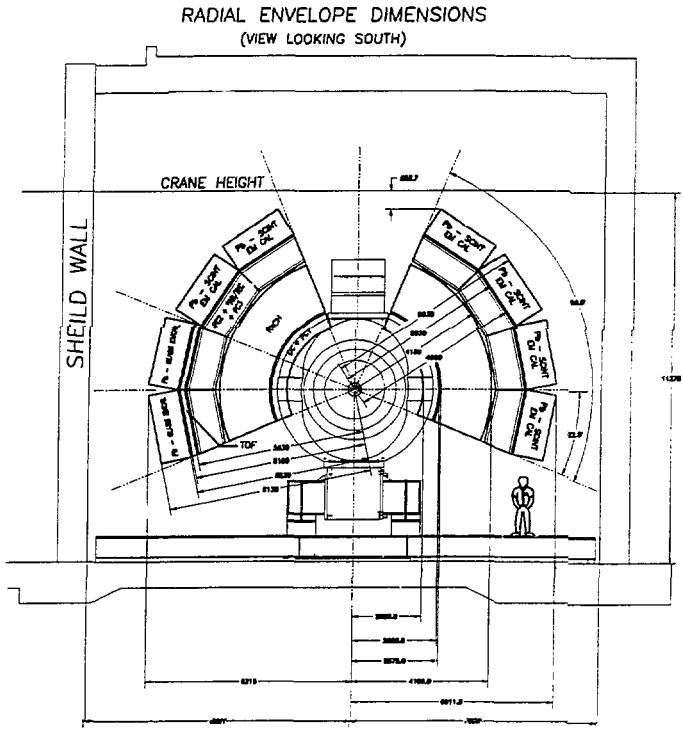

Figure 3: The Central Magnet modules shown arrayed around the beamline. The dimensions are in millimeters.

integral of ≈0.72 Tesla-meters at 15 degrees from the beam axis and decreasing at larger angles. The muons pass through this radial field for momentum and charge analysis.

Tracking System:

Drift Chambers: As a particle travels from the collision point outward it first encounters the drift chamber system, placed between r=2.05m and 2.45m, with η and ϕ coverage over the whole arm. There are 32 wire planes with wire directions either parallel to the z axis (which gives the ϕ information), or inclined at $\pm 5°$ to this

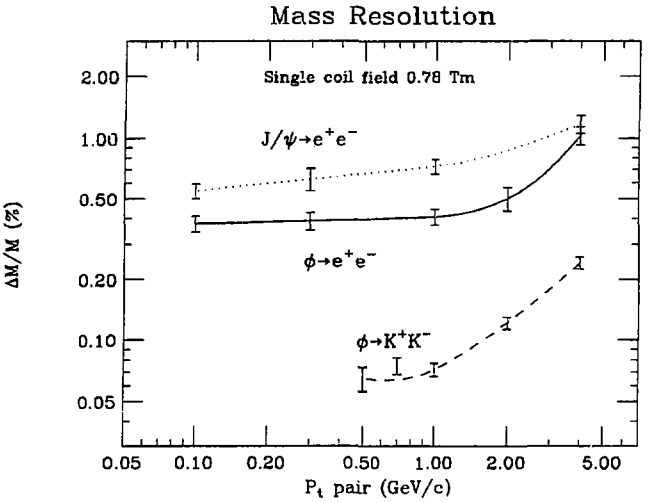

Figure 4: Mass resolution as a function of p_T for the ϕ and J/ψ.

direction (to give approximate information on the z coordinate). In addition to the cathode, field, and anode wires found in a conventional drift chamber, there are also channel wires and guard wires whose respective functions are to shape the cathode-to-anode drift field, and to block off the drift entirely from one side of the anode wire. Since drift electrons can now only approach the anode from one direction, the left-right ambiguities (and their combinatorics) inherent in conventional drift chambers no longer exist. The price for this is that the number of true hits is reduced by a factor of two, since every alternate wire will be blind to a given track. In an attempt to reduce the occupancy rate because of the long cell length in the z direction, instead of single wire from z=-1.8m to 1.8m there are two wires, one for positive z and one for negative, both terminated at z=0 on a thin support structure.

Pad Chambers: The tracking detectors that resolve the occupancy problem are the pad chambers. These are planar, and have the same acceptance/coverage as the drift chambers. There are 3 pad chambers, placed between the drift chambers and the RICH, between the RICH and the TEC, and again between the TEC and the TOF. On the surface of each are thousands of chevron-shaped pads, (each with its own electronic readout) providing the 3 dimensional location of a hit and crude time of flight information. The pad chambers require a large channel count, but our computer simulations have shown that it is necessary in the tracking system to have some detector with non-projective geometry to reduce combinatorics of hits when

doing pattern recognition. Also the pad chamber response is fast and can be used in triggering. Within each chevron pad unit there are cathode wires, and the chevron itself serves as anode, both in a gas volume. The pads are sized so that the signal covers a few pads, making it possible using a centroid, to calculate the hit position to an accuracy better than the pad size itself. In analysis the pads will provide track points to assist the drift chamber tracking. Since the occupancies expected in all 3 pad planes are similar, the chevron pad sizes in planes 2 and 3 are scaled up with their distance from the beamline, so that each of the planes has about 16000 channels.

TEC: The Time Expansion Chamber provides tracking information and particle identification, allowing e^-/π separation between 0.25 GeV/c and 3.0 GeV/c. It is placed with the inner and outer radii at 4.1m to 4.6m. In principle it is similar to a TPC. Within the chamber are a 3cm ionization volume filled with an argon gas mixture, a cathode wire plane, and an anode wire plane. A charged particle creates ionization sites in the gas and the resulting secondary electrons drift onto the anode wires. Fast clocked electronics digitize the drifting ionization signal in time slices so that position information and integrated charge can be extracted later. From this, track points and hence a short 3 dimensional track vector are reconstructed. The charge deposited is used for dE/dx estimate in the particle identification.

These three detectors working together form the Central Magnet tracking system. They are capable of a vector meson mass resolution which is better than 1% at all transverse momenta below 2 GeV/c. The mass resolution as a function of p_T is shown in Figure 4.

Ring Imaging Cerenkov:

The RICH is the primary device for identifying electrons. It is placed immediately behind the drift chambers, with inner and outer radii of 2.6m and 4.0m. Only $e^{\pm}$ (or pions with momentum greater than $\approx$4 GeV/c) will radiate Cerenkov photons. Large spherical mirrors on the outer face reflect this radiation to 4 arrays of 1 inch diameter photo-multiplier tubes (PMT) (two arrays for each arm, mounted on the pole-faces of the central magnet containing a total of 6400 tubes). The gas volume and pressure are chosen so that the number of photons is sufficient to make a ring image in the PMT array after various efficiencies and losses have been considered. A focussing mirror (Winston Cone) is mounted on each PMT, so that only photons incident from a restricted angular range can enter. It is then possible to approximately calculate the direction vector of an electron and associate it with a track measured more accurately from the drift chambers. The mirrors are constructed from a lightweight carbon fiber onto which a reflective surface is deposited.

Time of Flight:

The TOF system is a particle identification system for charged hadrons, whose main purpose is to differentiate between charged $\pi^{\pm}$ and $K^{\pm}$. It is an array of long scintillator slats oriented in the $r-\phi$ direction. A PMT is connected to the end of each slat. The array is located at r=5m from the beamline, between the TEC and the EMCal. By reading both PMT's one gets the particle time of flight and the position along the slat at which it passed through. Only a portion of one of the central

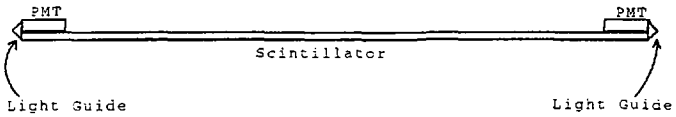

Figure 5: A typical Time of Flight array element.

arms is given TOF coverage. This is still sufficient to measure single charged particle production rates and also to reconstruct high p_T ϕ mesons decaying to K^+K^-. The time resolution of the slats is σ=80 pico-seconds. With this it can resolve 2.4 GeV/c π from K at a 4σ level. A typical TOF slat is shown schematically in Figure 5.

Electromagnetic Calorimeter:

The EMCal is located immediately behind the TOF wall. It is used to measure the energies of electrons and photons by causing them to form electromagnetic showers. Two different technologies are used. The EMCal is divided into 4 sections, two in each central arm. Three of these use modules composed of alternate layers of lead and scintillator, in which secondaries produced in lead produce light in scintillator. The fourth uses lead-glass modules in which Cerenkov light from electron induced showers is gathered. Hadrons too will deposit energy in the EMC, but generally this will be only minimum ionizing energy; much less than an electromagnetic shower. Even in the cases where a hadronic shower is produced, this has very different longitudinal and transverse profiles than an electromagnetic shower.

The Pb-scintillator portion will be 18 radiation lengths thick, with module faces square, 5.25cm to a side. This small size is needed to keep the occupancy low. A total of ≈18000 modules will be used. Wavelength shifting optical fibers will skewer each module longitudinally and light produced in the scintillator layers will find its way into the fibers and from there to the readout PMT's.

The Pb-glass modules are already built and are being used by the WA98 experiment at CERN. After that they will be given to Phenix. Each module presents a 4cm by 4cm face to the oncoming particles. The thickness is 40cm, 16 radiation lengths.

The EMCal will be used to provide a trigger for single, high-momentum electrons and photons, giving the particle energy, and modest time of flight information. A more global characterization of the event will also be made by looking at the total transverse electromagnetic energy of the whole event.

Muon Detector:

The muon detector is located behind one of the central magnet pole faces and has complete azimuthal coverage about the beam line, from polar angle θ=10° to 35°. The major physics goal is to measure the $\mu^{\pm}$ pairs that result from the decays of the J/ψ, ψ' and Υ mesons, as well as from the Drell-Yan process. The problem faced here is to identify and measure relatively few muons from among a large number of

charged hadrons. Since the μ and π are very close in mass (0.106 GeV and 0.139 GeV respectively), techniques like time of flight measurement and Cerenkov discrimination will not work. There is also a large background of muons from π decay. The main components of the muon detector are (starting from the collision point) a copper cone mounted on the inner side of the central magnet poleface, the poleface itself, 3 tracking chambers in a radial magnetic field formed by the muon magnet and the muon identifier, composed of several layers of shielding and streamer tube detectors. These function as follows: The purpose of the copper cone is to slow down or destroy $\pi^{\pm}$ before they have a chance to decay to muons, since once formed, a decay muon is almost impossible to distinguish from one in which we are interested. The cone extends as close as possible to the central collision point as can be done without creating extra backgrounds that affect the central arm detectors. The cone and poleface are also used to reduce the number of hadrons that reach the drift chamber tracking system. The intent here is to reduce them only to the point where the hit combinatorics can be resolved by our pattern recognition programs and tracks can be accurately measured. This is because muons too suffer energy loss and multiple-scattering as they pass through the shielding, and we want the degradation of their momentum measurement to be minimized. There are 3 drift chamber stations that sit in the muon arm magnetic field. Downstream of these is the muon identifier. These are streamer tube detectors arrays placed behind steel absorber walls. It is here that the same tracks that were momentum measured in the drift chambers are checked for penetrability. Muons will be more penetrating, and also will produce only one bit per streamer tube whereas hadrons will interact, shower, and produce multiple hits. At this point the multiple scattering and energy loss effects of the shielding are not so important as we already have the momentum measurement. It is only necessary to follow the particle through and associate it with a track measured in the drift chambers upstream.

The Inner Detectors:

Phenix contains a set of detectors close to the central collision point to provide the position of the collision point, a time of flight start signal, multiplicity measurements, and a multiplicity trigger. The inner detectors consist of a silicon based Multiplicity Vertex Detector (MVD) and Cerenkov based beam-beam counters (BBC).

The MVD has two concentric hexagonal barrels about the beamline with an end-cap at each end. The barrel radii are 5cm and 8cm, and they are composed of Si strips of length 5cm and 8cm respectively, with a strip pitch of 200μm. The endcaps are disk-shaped and here the Si is in the form of pads, ranging from 2mm per side squares near the beam to 5mm squares at the outer edges. Both the strips and the pads will be used for multiplicity measurements, with η coverage ± 2.7. The strips will also be used for the collision vertex determination, which the Phenix computer simulation packages (Pisa/Pisorp) show can be done to 165μm in AuAu collisions.

The BBC elements are Cerenkov detectors, with quartz radiators glued to PMT's and arranged in concentric rings around the beamline. The goal is to achieve 100ps timing resolution for the time of interaction. If the difference of times from the BBC's at either end is taken the position of the collision vertex can be obtained to $\sim$2cm

and can be used for the first level trigger. This information will be used by other detectors and higher level triggers as well.

Summary

Phenix is well on its way to being a fully designed, workable, experiment. Over the next few years detector R & D will continue, to be gradually replaced by actual construction. When the accelerator and detector turn on later this decade, we expect to be able to sustain a high event rate and explore the newly opened realm of ultra high energy and matter densities that has been made available to us.

Acknowledgments

The authors would like to thank the *PHENIX* collaboration for their computer simulation and R&D efforts and for many hours of stimulating conversation and diversion.

This work was performed at LLNL under DOE contract W-7405-ENG-48.

References

[1] K.Kajantie, J.Kapusta, L.McLerran, and A.Mekjian, Phys.Rev.D34, 2746 (1986).

[2] D.Lissauer and E.V.Shuryak, Phys.Lett.B253, 15 (1991).

[3] A.Shor, Phys.Rev.Lett.54, 1122 (1985).

[4] T.Matsui and H.Satz, Phys.Lett.B178, 416 (1986).

[5] P.V.Ruuskanen, Nucl.Phys.A544, 169c (1992).